



Expression of the unconventional myosin Myo1c alters sodium transport in M1 collecting duct cells

Mark C. Wagner, Bonnie L. Blazer-Yost, Judy Boyd-White, Anjaiah Srirangam, Janice Pennington and Stacy Bennett

Am J Physiol Cell Physiol 289:120-129, 2005. First published Feb 16, 2005;
doi:10.1152/ajpcell.00569.2003

You might find this additional information useful...

This article cites 53 articles, 32 of which you can access free at:

<http://ajpcell.physiology.org/cgi/content/full/289/1/C120#BIBL>

This article has been cited by 2 other HighWire hosted articles:

Interaction of epithelial ion channels with the actin-based cytoskeleton

C. Mazzochi, D. J. Benos and P. R. Smith

Am J Physiol Renal Physiol, December 1, 2006; 291 (6): F1113-F1122.

[Abstract] [Full Text] [PDF]

Redistribution of Myosin VI from Top to Base of Proximal Tubule Microvilli during Acute Hypertension

L. E. Yang, A. B. Maunsbach, P. K.K. Leong and A. A. McDonough

J. Am. Soc. Nephrol., October 1, 2005; 16 (10): 2890-2896.

[Abstract] [Full Text] [PDF]

Updated information and services including high-resolution figures, can be found at:

<http://ajpcell.physiology.org/cgi/content/full/289/1/C120>

Additional material and information about *AJP - Cell Physiology* can be found at:

<http://www.the-aps.org/publications/ajpcell>

This information is current as of December 13, 2006 .

Expression of the unconventional myosin Myo1c alters sodium transport in M1 collecting duct cells

Mark C. Wagner,¹ Bonnie L. Blazer-Yost,² Judy Boyd-White,¹†
Anjaiah Srirangam,¹ Janice Pennington,¹ and Stacy Bennett¹

¹Department of Medicine, Indiana University School of Medicine, and ²Department of Biology, Indiana University-Purdue University at Indianapolis, Indianapolis, Indiana

Submitted 15 December 2003; accepted in final form 11 February 2005

Wagner, Mark C., Bonnie L. Blazer-Yost, Judy Boyd-White, Anjaiah Srirangam, Janice Pennington, and Stacy Bennett. Expression of the unconventional myosin Myo1c alters sodium transport in M1 collecting duct cells. *Am J Physiol Cell Physiol* 289: C120–C129, 2005. First published February 16, 2005; doi:10.1152/ajpcell.00569.2003.— Epithelial cells rely on proper targeting of cellular components to perform their physiological function. This dynamic process utilizes the cytoskeleton and involves movement of vesicles to and from the plasma membrane, thus traversing the actin cortical cytoskeleton. Studies support both direct interaction of actin with channels and an indirect mechanism whereby actin may serve as a track in the final delivery of the channel to the plasma membrane. Actin-dependent processes are often mediated via a member of the myosin family of proteins. Myosin I family members have been implicated in multiple cellular events occurring at the plasma membrane. In these studies, we investigated the function of the unconventional myosin I Myo1c in the M1 mouse collecting duct cell line. Myo1c was observed to be concentrated at or near the plasma membrane, often in discrete membrane domains. To address the possible role of Myo1c in channel regulation, we expressed a truncated Myo1c, lacking ATP and actin domains, in M1 cells and compared electrophysiological responses to control M1 cells, M1 cells expressing the empty vector, and M1 cells expressing the full-length Myo1c construct. Interestingly, cells expressing the Myo1c constructs had modulated antidiuretic hormone (ADH)-stimulated short-circuit current and showed little inhibition of short-circuit current with amiloride addition. Evaluation of enhanced green fluorescent protein-Myo1c constructs supports the importance of the IQ region in targeting the Myo1c to its respective cellular domain. These data are consistent with Myo1c participating in the regulation of the Na⁺ channel after ADH stimulation.

actin; cytoskeleton; ion channel; kidney

KIDNEY EPITHELIAL CELLS perform diverse functions that are dependent on their polarized structure and targeting of proteins to specific cellular domains (10). The regulated and dynamic organization of the apical and basolateral membrane domains relies, in part, on the actin cytoskeleton. The presence of an intricate actin network in close proximity to the plasma membrane enables actin and its associated proteins to actively participate in the regulation of membrane events in epithelial cells (11, 33, 45, 46). Disruption to the actin cytoskeleton occurs during ischemia and other disease processes and contributes to altered epithelial cell structure and function (56).

Modulation of actin structure and actin-dependent processes is often mediated via members of the myosin family of proteins. Myosin I proteins contain ATP-, actin-, and membrane-

binding domains that make them excellent candidates to regulate exocytotic and endocytotic events as well as to serve as participants in the regulation of integral membrane proteins such as channels (2). Support for an active role of myosin I and other myosins in these processes exists in multiple systems (12, 15, 17, 49).

We previously identified (9) Myo1c, previously called myosin I β or Myr2, as a myosin I enriched in the brush border of proximal tubule cells. After an ischemic insult that caused the collapse of the actin-rich brush border, Myo1c was found in cellular blebs and urine. Its return to the brush border, as observed by immunofluorescence, occurred after the structural recovery of the actin in the brush border. Interestingly, Myo1c was observed to be present in most, if not all, kidney tubules, including the collecting duct.

The ubiquitous distribution of Myo1c suggests that it likely participates in fundamental cell functions. Research from several laboratories supports the contention that Myo1c is the best candidate for the adaptation motor of hair cells (21). This process depends on interactions between actin and an ion channel located in the apical portion of stereocilia. A more recent study suggests that depletion of Myo1c from adipocytes, with small interfering RNA, reduces the transport of Glut4-containing vesicles to the plasma membrane (7). These studies implicate Myo1c in actin-associated functions at the cortex of various cell types.

The kidney collecting duct's primary function is to make final adjustment of urinary solute osmolarity and concentrations (43). These tubules consist of two functionally distinct epithelial cells—the principal and intercalated cells. The principal cells respond to antidiuretic hormone (ADH) or vasopressin by transporting aquaporin channels to the apical membrane. Vasopressin also stimulates the epithelial Na⁺ channel ENaC, present in principal cells. Data from several laboratories support the idea that ENaC is inserted from a cytoplasmic pool after ADH stimulation (5, 18, 48). In addition, a role for the cortical actin cytoskeleton has also been shown. Cl⁻ channels including CFTR are also present in both principal and intercalated cells and in M1 cells (30, 31, 45, 53). The mechanism(s) that is used to regulate CFTR's Cl⁻ transport and its interactions with other channels including ENaC is complex and involves both trafficking and regulatory components (4).

By immunofluorescence, Myo1c is seen to be concentrated at the plasma membrane in M1 cells. We hypothesized that ENaC channel insertion depends on actin-myosin interactions

† Deceased 17 April 2003.

Address for reprint requests and other correspondence: M. Wagner, Indiana Univ. School of Medicine, Dept. of Medicine/Nephrology, 950 West Walnut St., R2-202, Indianapolis, IN 46202 (e-mail: wagnerm@iupui.edu).

The costs of publication of this article were defrayed in part by the payment of page charges. The article must therefore be hereby marked "advertisement" in accordance with 18 U.S.C. Section 1734 solely to indicate this fact.

and that disruption of Myo1c would adversely affect the normal ion transport response after ADH stimulation of M1 cells. To test our hypothesis, we created a truncated Myo1c lacking both ATP and actin domains and stably expressed this construct in M1 cells. Evaluation of ion transport responses is consistent with Myo1c having a role in ENaC activation via channel delivery and/or insertion into the plasma membrane.

MATERIALS AND METHODS

Materials. The hormones, agonists, and inhibitors used in these experiments were ADH ([Arg⁸]-vasopressin; Sigma, St. Louis, MO); amiloride hydrochloride (Sigma); dibutyryl adenosine 3',5'-cyclic monophosphate (DBcAMP; Sigma); 5-nitro-2-(3-phenylpropylamino) benzoic acid (NPPB; Biomol Research, Plymouth Meeting, PA); and niflumic acid and tamoxifen (EMD Biosciences, San Diego, CA). Monoclonal antibodies against Myo1c were described and characterized previously (9, 22, 54, 55). In addition, we also used a polyclonal antibody against Myo1c (gift of Drs. Joseph Albanesi and Barbara Barylko, University of Texas Southwestern) for immunofluorescence. Fluorophore-conjugated secondary antibodies were from Jackson ImmunoResearch (West Grove, PA), and Alexa 488 phalloidin was from Molecular Probes (Eugene, OR). The ZO-1 antibody (R26.4C) developed by Dr. D. A. Goodenough was obtained from the Developmental Studies Hybridoma Bank developed under the auspices of the National Institute of Child Health and Human Development and maintained by the Department of Biological Sciences, University of Iowa (Iowa City, IA).

Cell culture. The M1 cell line, originally developed by Dr. G. Fejes-Toth (50), was obtained from the American Type Culture Collection (Manassas, VA). Cultures were routinely grown on plastic in DMEM-Ham's F-12 medium with L-glutamine and 15 mM HEPES supplemented with 2.5% Cosmic calf serum (HyClone, Logan, UT), 2.5% fetal bovine serum, 100 U penicillin, and 100 µg/ml streptomycin. Costar Transwell polycarbonate filters, 0.4-µm pore size, were used for electrophysiological assays and some immunofluorescence experiments. Cells were used on days 20–22 after seeding onto filters (2 × 10⁵ cells/cm²) for Ussing chamber experiments.

Construction of Myo1c constructs. Standard molecular techniques were used to create a truncated Myo1c construct, which was inserted into the pcDNA6/V5-His plasmid (Invitrogen, Carlsbad, CA). PCR was used to amplify a Myo1c tail construct that contained all the IQ motifs (start nucleotide 2289). The template DNA was the full-length rat Myr2 construct from Dr. Martin Bahler, University of Münster, Germany (42), and the two primers used were the following: forward 5'-CTGGATCCATGGGCAGGACTAAGATC-3' and reverse 5'-AGGACACCTAGTCAGACAAAATGATGC-3'. The forward primer contained a BamHI site and the 3' end of the construct an EcoRI site that were subsequently cut to enable ligation with pcDNA6/V5-His plasmid cut with BamHI-EcoRI. Proper placement was verified by DNA sequencing of the Myo1c IQ tail pcDNA6/V5-His construct (Myo1cIQ). Similar methods were used to place the full-length Myr2 construct into pcDNA6/V5-His plasmid. M1 cells were transfected with Myo1cIQ, Myo1cFL, or pcDNA6/V5 lacking any insert with Lipofectamine (Life Technologies, Rockville, MD), and expressing cells were selected with blasticidin (10 µg/ml). Two rounds of selection were performed with cloning rings. M1 cells stably expressing the Myo1c IQ construct (M1IQ) or Myo1cFL construct (MF3) are maintained in blasticidin (4 µg/ml) containing medium, and express the truncated Myo1c at levels of ~25% of the endogenous Myo1c, based on immunoblot. Identification of the Myo1c constructs was accomplished by Western blotting with either Myo1c or V5 antibodies. We have been unable to label the Myo1c constructs by immunofluorescence with either V5 or His antibodies. Construction of enhanced green fluorescent protein (EGFP)-Myo1c plasmids also used the full-length Myr2 construct as starting template to place the

full-length, IQ (lacking ATP- and actin-binding domains), and Tail (lacking ATP-, actin-, and first 3 IQ domains; Ref. 16) Myr2 constructs into the appropriate version of pEGFP-C from Clontech (Palo Alto, CA). Briefly, full-length Myr2 was cut with EcoRI and ligated into pEGFP-C2 cut with EcoRI. With similar methods Myo1c constructs lacking ATP- and actin-binding domains, IQ-EGFP (start nucleotide 2289), and T-EGFP (start nucleotide 2595), which lacks ATP, actin, and IQ motifs, were constructed. EGFP for all three constructs was placed on the amino end and confirmed by sequencing. A diagram of these constructs and their respective domains is presented in Fig. 1.

Western blot analysis. SDS-PAGE was carried out with Bio-Rad Criterion Tris·HCl gels (Hercules, CA), Fisher PAGER gold precast gels (Hanover Park, IL), or Invitrogen gels. Proteins were transferred by electroblotting to Millipore polyvinylidene difluoride at 100 V for 30–60 min with cooling in 5% methanol-10 mM 3-(cyclohexylamino)-1-propanesulfonic acid (CAPS), pH 11. Membranes were blocked for 2 h with a proprietary blocking solution (Amersham Liquid Block) diluted to 5% with PBS (150 mM NaCl and 70 mM sodium phosphate, pH 7.4) (58). This was followed by incubation with primary antibodies for 2 h in blocking solution followed by three to five washes in PBS + 0.3% Tween 20. Horseradish peroxidase-conjugated secondary antibodies from Jackson ImmunoResearch were diluted 1:10,000 in blocking solution and incubated for 1 h, followed by five additional washes with PBS-Tween 20. Detection of bound antibodies was performed with a Pierce (Rockford, IL) enhanced chemiluminescence kit according to the manufacturer's instructions.

Triton X-100 extraction of cells was performed with the following buffer (in mM): 50 imidazole, 50 KCl, 0.5 MgCl₂, 0.1 EDTA, 1 EGTA, and 1 DTT with 1% Triton X-100 and protease, kinase, and phosphatase inhibitors. Cells on filters were rapidly cooled, scraped, and pelleted in cold Krebs buffer. The pellet was extracted for 10–15 min on ice with the above buffer, followed by centrifugation for 30 min at 100,000 g in a Beckman table top ultracentrifuge (rotor 120.1). Pellets and supernatants were made equal volume with sample buffer and analyzed by Western blotting. Quantitation of Western blots was performed with UN-SCAN-IT (Silk Scientific, Orem, UT) digitizing software.

Immunofluorescence. Fixation and immunolabeling of kidney sections was performed as described previously (9). Briefly, rat kidneys were perfused fixed according to the procedure of Maunsbach and Afzelius (36). Fifty- to one hundred-micrometer sections were obtained with a vibratome. Tissue was permeabilized, with either 1% SDS or 1% Triton X-100, for 5 min, followed by antibody labeling. Myo1c primary antibodies were used (5–10 µg/ml), and secondary antibodies were conjugated to Cy5 (Jackson ImmunoResearch) or Alexa dyes (Molecular Probes). F-actin was labeled by including Alexa 488 or Oregon Green phalloidin (Molecular Probes) diluted 1:200 with the secondary antibody.

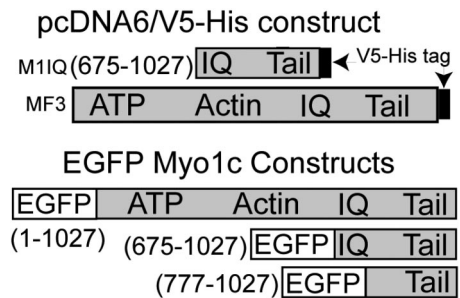


Fig. 1. Myo1c constructs used in transfection experiments. Each construct was created from the full-length rat Myr2 plasmid. The amino acids of each construct are shown in parentheses along with their major domains. The V5-His tag is located on the carboxy end, whereas enhanced green fluorescent protein (EGFP) is present on the amino terminus.

Glass- or filter-grown cells were fixed with 2–4% paraformaldehyde and permeabilized with either 0.5% Triton X-100 or 0.05% saponin in PBS. Immunolabeling for all antibodies was performed as previously described, using the Myo1c antibodies (54, 55).

Transient transfection. Cells were plated onto Mattek (Ashland, MA) coverslip dishes and transfected with either Effectene (Qiagen, Valencia, CA) or Lipofectamine 2000 (Life Technologies) according to the manufacturer's instructions. Transfected cells were imaged live with the Zeiss LSM 510 confocal microscope and a $\times 60$, 1.4-numerical aperture (NA) water objective. Temperature and pH were controlled by use of a Warner warm stage holder and placement of cells into a HEPES-Krebs buffer (in mM: 1 $MgCl_2$, 1 $CaCl_2$, 55 NaCl, 3 KCl, 10 dextrose, 10 HEPES, and 150 sucrose).

Microscopy. Images were collected with either a MRC-1024 laser scanning confocal microscope (Bio-Rad) or a Zeiss LSM 510 confocal microscope at the Indiana Center for Biological Microscopy. In both cases, high-NA objectives were used. Z stacks were collected with a step size between 0.2 and 0.5 μm . Selected images were imported into Adobe Photoshop and labeled with Adobe Illustrator.

Electrophysiological studies. Cells were grown for 20–22 days on 2.5-cm Falcon Transwell polycarbonate filters or Snapwells. The filters were clamped between the halves of an Ussing chamber (World Precision Instruments, Sarasota, FL) (30). The fluid chamber was maintained at 37°C with a water-jacketed buffer reservoir. pH was maintained and buffer circulated with a 5% CO_2 -95% O_2 gas lift. The electrodes were connected to a voltage-clamp amplifier (current voltage clamp; World Precision Instruments) for measurement of net ion flux as monitored under short-circuit conditions [short-circuit current (SCC)] (28). Transepithelial resistance was calculated by intermittently applying a 2-mV pulse across the epithelium and measuring the resultant deflection in SCC.

Serum-free DMEM-F-12 medium was used for studies shown in Figs. 4–6. Filters were placed into the chambers and incubated under SCC conditions until a steady baseline was obtained (0.5–1 h). Concentrations and times of addition of the various compounds are indicated in Figs. 4–6. Each experiment was performed with matched cultures grown in parallel.

RESULTS

Myo1c is concentrated at plasma membrane in collecting duct cells. Our previous studies (9, 55) focused on the distribution of Myo1c in proximal tubule cells and the effects of in vitro and in vivo ischemia. Those studies indicated that Myo1c was present in most, if not all, the kidney tubules. The goal of the present studies was to characterize the distribution of Myo1c in a collecting duct cell line and to address its function by expressing the dominant-negative tail of Myo1c in these cells. Figure 2 contains confocal images of 50- to 100- μm rat kidney sections labeled with Myo1c antibody or phalloidin. Figure 2, A–C, show that Myo1c is concentrated in the apical region of distal or collecting duct cells. Figure 2, C and D, are two pictures of the same double-labeled section showing considerable colocalization of Myo1c and F-actin.

To begin to address the function of Myo1c in distal tubule cells we used the M1 mouse collecting duct cell line. These cells have properties of both principal and intercalated cells (29, 50). A Myo1c construct lacking ATP- and actin-binding domains was created and stably expressed in M1 cells (M1IQ). The absence of ATP- and actin-binding domains prevents this construct from performing actin-dependent mechanochemical activities, thus having the potential to act as a dominant-negative construct. This approach has been used successfully for several unconventional myosins (12, 14, 15, 17, 49).

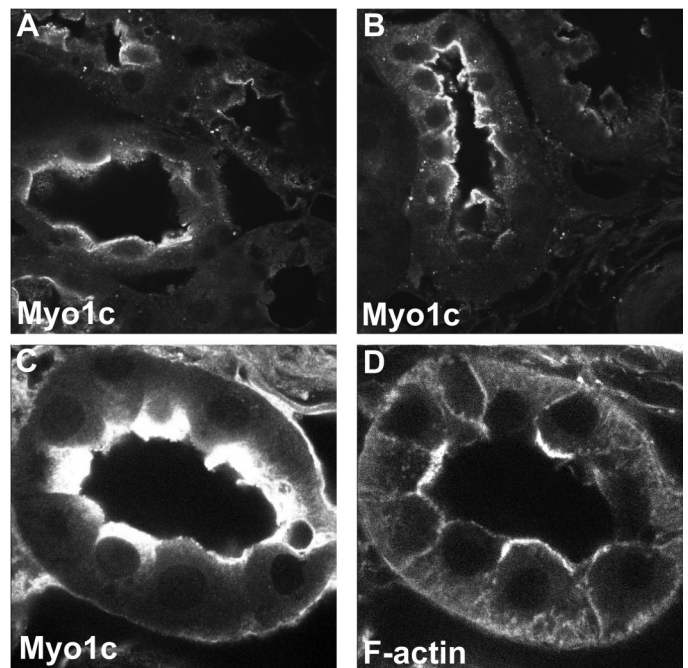


Fig. 2. Myo1c is concentrated in proximity to the apical plasma membrane in collecting duct cells. Fifty- to one hundred-micrometer rat kidney sections were imaged with a Bio-Rad confocal microscope; single planes are shown. A–C: Myo1c is concentrated in the apical region of distal or collecting duct cells. C and D were double labeled, with D showing the location of F-actin with fluorophore-conjugated phalloidin.

The first question addressed with the M1 cells was Myo1c localization and the effect of expression of the Myo1c IQ construct on endogenous Myo1c's distribution and F-actin structure. Figure 3 shows the location of Myo1c in M1 and M1IQ cells grown on filters. Both x - y planes and x - z cross sections (apical membrane at top) are presented. X - z images show only Myo1c location. The concentration of Myo1c at the apical and lateral membranes is seen in both M1 and M1IQ cells. The arrows in x - z sections point to areas containing a high concentration of Myo1c, which may correspond to special membrane/cytoskeletal domains. No significant difference was observed in Myo1c location or the actin cytoskeleton in parental M1 cells or M1IQ cells expressing the truncated Myo1c construct. The presence of Myo1c near the plasma membrane, often in distinct domains, is consistent with this myosin having a role in membrane events such as channel regulation. Myo1c location in M1C and MF3 cells was comparable to that in M1 and M1IQ cells (data not shown).

Expression of truncated Myo1c alters cell responses that require ion channel function. In light of Myo1c's ubiquitous tissue distribution and known functions, we hypothesized that this unconventional myosin participates in the regulation of ion channels in kidney tubules. As a test of this hypothesis, we evaluated changes to ADH stimulation of Na^+ channels, a well-characterized process occurring in these cells that likely involves both channel insertion and activation. This possibility was addressed by monitoring ion transport in intact epithelial monolayers with the electrophysiological method of SCC in parental M1 cells and M1IQ cells.

Figure 4 shows the response for both the parental M1 cells and the M1IQ cells that contain both endogenous Myo1c and

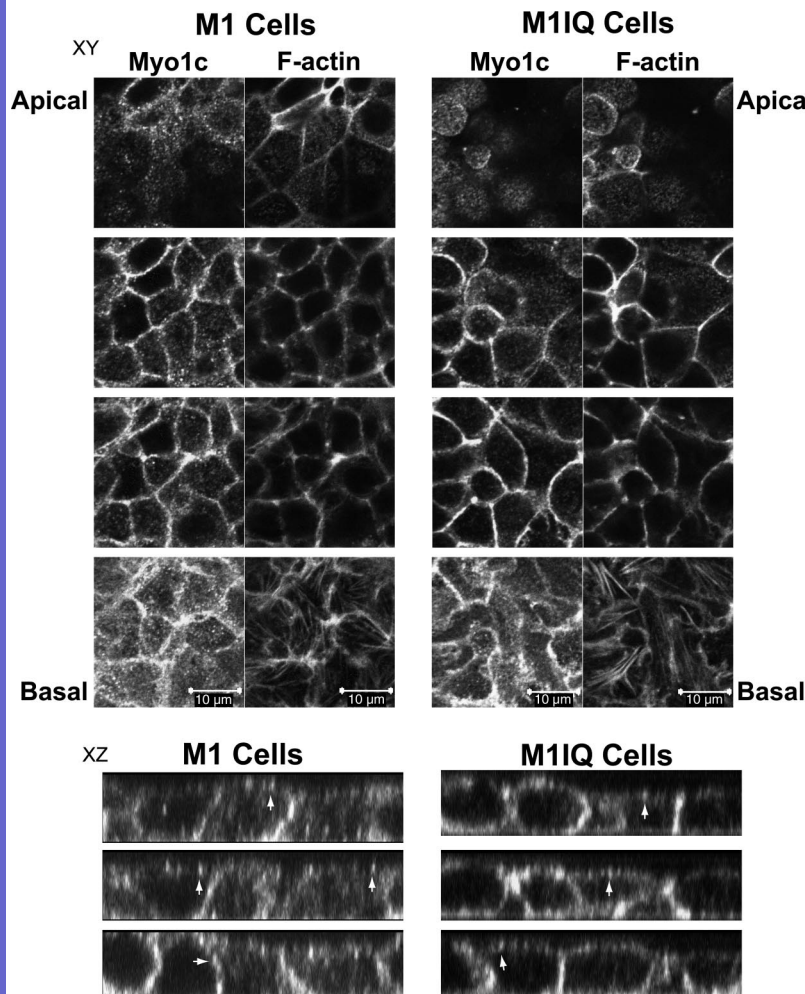


Fig. 3. Location of Myo1c in M1 and M1IQ cells grown on permeable supports. Cells were grown for 4–10 days under conditions identical to those used for electrophysiological analysis. Filters were fixed, permeabilized with Triton X-100, and reacted with Myo1c monoclonal antibody, followed by a Cy5-conjugated secondary antibody and Alexa 488 phalloidin to label F-actin. A Zeiss LSM 510 confocal microscope was used to collect all images. Four image planes, apical to basal, were selected to encompass representative cross-sectional areas of the cells. Both *x-y* planes and *x-z* cross sections (apical membrane at top) are presented. *x-z* Images show only Myo1c location. Bar = 10 μm . Note the concentration of Myo1c at the apical and lateral membrane in both M1 and M1IQ cells as well as the colocalization of Myo1c and F-actin in many locations. As we have observed in other cells, Myo1c does not colocalize with F-actin in stress fibers. Arrows in *x-z* sections point to some of the regions containing a high concentration of Myo1c, which may correspond to special membrane/cytoskeletal domains. No significant difference was observed in the actin cytoskeleton between parental and transfected cells.

truncated Myo1c lacking ATP and actin domains. There was a diminished response of the M1IQ cells to ADH and an apparent reduction of amiloride-sensitive transport in these cells. These results are consistent with a reduced delivery and/or activation of ENaC. The subsequent addition of DBcAMP resulted in an amplified response for the M1IQ cells in the presence of the Na^+ channel inhibitor amiloride. The amplified DBcAMP response in the M1IQ cells suggests that a Cl^- channel may be affected. A reciprocal activation arrangement between ENaC and CFTR has been observed in M1 cells (31) and other cell types (35, 45). Differences between cell types were statistically significant.

To further substantiate the participation of Myo1c in the ADH/ Na^+ channel response, we created M1 cells expressing the full-length Myo1c (MF3). Recent data suggest that overexpression of Myo1c promotes membrane fusion (8); thus these cells may have increased delivery of membrane proteins including channels. In Fig. 5A, M1 and M1IQ cells were analyzed, along with MF3 cells, using electrophysiological techniques on confluent monolayers. As in Fig. 4, there was a diminished ADH response, minimal to no amiloride effect, and increased cAMP response in the M1IQ cells compared with the M1 parent line. Interestingly, MF3 cells have a significantly increased basal SCC that is also not responsive to ADH or amiloride but responds to cAMP like the M1IQ cells. Thus

whether truncated Myo1c is expressed or increased expression of full-length Myo1c occurs, a diminished ADH response and much-reduced amiloride inhibition are observed. The increase in SCC observed in the MF3 cells may be the result of increased channel density or activation. In Fig. 5B M1 cells expressing the empty pcDNA6/V5-His plasmid (M1C) were compared with M1 cells, and no significant differences were observed. The average peak ADH response was 8 $\mu\text{A}/\text{cm}^2$ for M1 cells and 5.9 $\mu\text{A}/\text{cm}^2$ for M1C cells. The average peak cAMP response was 9.1 $\mu\text{A}/\text{cm}^2$ for M1 cells and 7.1 $\mu\text{A}/\text{cm}^2$ for M1C cells. As in Fig. 5A these cells were run on the same day under identical conditions, using cells grown in parallel.

Figures 4 and 5 support the idea that manipulation of the Myo1c protein alters the normal ADH Na^+ channel response. To test this another way, we evaluated the changes to M1, M1IQ, and MF3 cells by treating cells with amiloride followed by ADH and cAMP (Fig. 6). As expected, the M1 cells have a significant decrease in SCC when amiloride is added; however, the M1IQ and MF3 cells have minimal if any inhibition by amiloride, as expected if ENaC is not contributing to the SCC. ADH has a minimal effect on ion transport in MF3 and M1IQ cells, whereas addition of DBcAMP again shows a dramatic increase in these cells. These results are consistent with ENaC unresponsiveness and increased Cl^- transport, possibly via

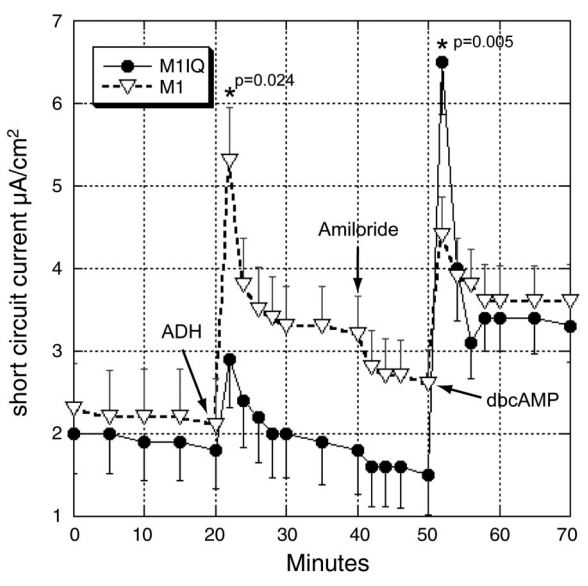


Fig. 4. Ion transport responses to increases in intracellular cAMP in control M1 and M1IQ cells expressing a truncated Myo1c. Antidiuretic hormone (ADH; 100 mU/ml) was added to the basal media at $t = 20$ min. Amiloride (10 μ M) was added to the apical media at 40 min, followed by 1 mM dibutyryl adenosine 3',5'-cyclic monophosphate (DBcAMP) added to the basal media at 50 min. Note the diminished response of the M1IQ cells to ADH and the amplified response to DBcAMP in the presence of the Na^+ channel inhibitor amiloride. Each data point represents $n = 6$ or 7. Points are means \pm SE; P values were calculated with an unpaired Student's t -test. Differences between cell types were statistically significant (*) at the peak response as indicated.

CFTR, occurring in the M1IQ cells that contain the truncated Myo1c and MF3 cells overexpressing Myo1c.

To begin characterization of the increase in ion transport observed after DBcAMP addition, we evaluated the effects of three Cl^- channel inhibitors on the DBcAMP response in the M1IQ cells (23, 26, 37, 44). These studies used a defined bath solution on both the apical and basolateral sides of the cells (in mM: 140 Na^+ , 4 K^+ , 1 Ca^{2+} , 1 Mg^{2+} , 124 Cl^- , 24 HCO_3^- , and 5 D-glucose) (24). The Cl^- channels targeted were CFTR, swelling-activated Cl^- ($I_{\text{Cl,swell}}$), and Ca^{2+} -activated Cl^- . Niflumic acid has a higher affinity for the Ca^{2+} -activated Cl^- channel than either the $I_{\text{Cl,swell}}$ or CFTR channels, whereas tamoxifen is classified as a $I_{\text{Cl,swell}}$ channel inhibitor (44). Neither niflumic acid (50 μ M) nor tamoxifen (50 μ M) inhibited DBcAMP-stimulated current increase in the presence of amiloride (data not shown). NPPB (100 μ M) completely inhibited the response. The inhibition by NPPB supports a role for Cl^- channels and, combined with the other inhibitor results, points to CFTR, whose presence in these cells is suggested by electrophysiology studies (31) and was shown by RT-PCR experiments (53). Additional evidence that Cl^- transport accounts for the SCC after DBcAMP addition came from studies using low- Cl^- buffers that showed an absent or much-reduced SCC change after DBcAMP (data not shown).

Measurement of resistances in the M1 parent line (1,134 \pm 58 Ω/cm^2 ; $n > 10$) vs. MC1, M1IQ, and MF3 cells showed that M1 cells and MC1 cells have essentially identical resistances. In contrast, the M1IQ cell resistance was more variable, always less than one-half of that of M1 and most often $\sim 220 \Omega/\text{cm}^2$. The MF3 cells had the lowest resistance, which was 34 \pm 24 Ω/cm^2 ($n > 10$).

Does expression of truncated Myo1c alter actin association as monitored by Triton X-100 extraction? Several studies suggest that myosin I can self-associate, possibly through tail-tail interactions (20, 38, 55). Given the similarity in Myo1c immunofluorescent staining in M1 and M1IQ cells, observed by using the Myo1c M2 antibody that recognizes both full-length and IQ truncated forms, it is reasonable to propose that the truncated form incorporates into endogenous Myo1c complexes. In these experiments three questions were addressed. First, does the incorporation of truncated Myo1c alter the Triton X-100 extractability of endogenous Myo1c? Second, does addition of DBcAMP alter Myo1c Triton X-100 extraction properties? Third, is the truncated Myo1c construct extracted with Triton X-100?

Filter-grown cells were extracted under control conditions and after addition of 1 mM DBcAMP for 2 min. Figure 7 shows the results from Western blots that were scanned and quantitated. The total quantity of Myo1c (pellet + supernatant) was set at 100%, and the percentage present in the supernatant, Triton soluble, is shown in the absence (Fig. 7, A, C, and E) and presence (Fig. 7, B, D, and F) of DBcAMP. There was a significant shift of Myo1c to increased solubility when the truncated Myo1c IQ construct was present (compare Fig. 7A

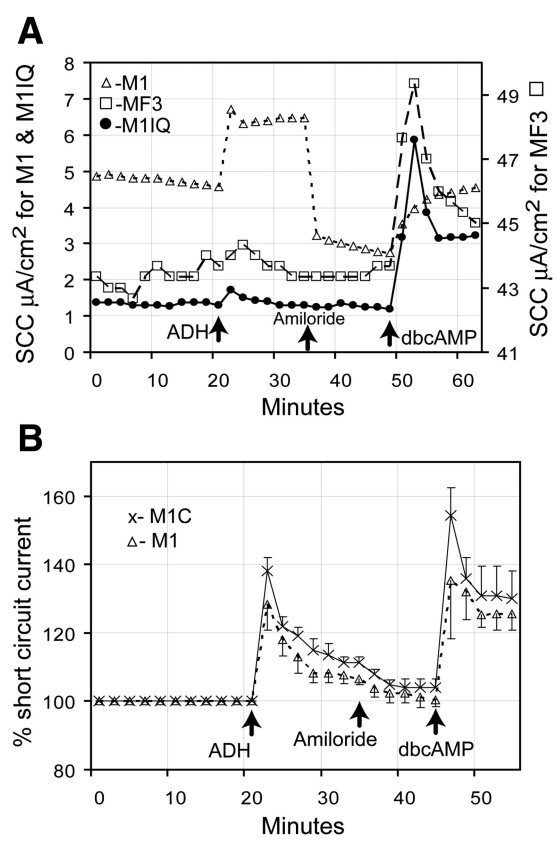


Fig. 5. A: ion transport responses in M1, M1IQ, and MF3 cells run in parallel after ADH, amiloride, and DBcAMP addition. Cells were grown and reagents added as in Fig. 4. Each data point represents the mean of 3 filters. Note the lack of ADH and amiloride response in the M1IQ and MF3 cells compared with the M1 parent line. SCC, short-circuit current. B: ion transport responses in M1 and M1C cells run in parallel after ADH, amiloride, and DBcAMP addition. Each data point represents the mean of 3 filters, and the error bars represent the average of the absolute deviations. Note the similarity in their responses.

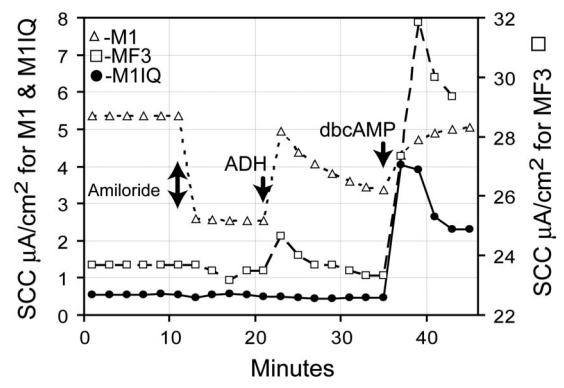


Fig. 6. Ion transport responses in M1, M1IQ, and MF3 cells run in parallel after amiloride, ADH, and DBcAMP addition. Cells were grown and reagents added as in Fig. 4. Each data point represents the mean of 3 filters. Note the lack of an amiloride response and diminished ADH response in the M1IQ and MF3 cells compared with the M1 parent line.

with Fig. 7C; $P = 0.021$, unpaired Student's t -test). The addition of DBcAMP to control M1 cells also triggered an apparent rearrangement that resulted in more Myo1c being Triton X-100 extractable (compare Fig. 7A with Fig. 7B). The variability between M1 filters is greater than in the M1IQ cells, and the P value by paired Student's t -test comparing Fig. 7A to Fig. 7B was 0.056. No difference was observed between the M1IQ cells after DBcAMP addition (compare Fig. 7C with Fig. 7D). Figure 7, E and F, show that the truncated Myo1c construct is $\sim 90\%$ Triton X-100 soluble, with the addition of DBcAMP causing no change.

Localization and targeting of EGFP-Myo1c constructs in M1 cells. Immunofluorescence results (Fig. 3) suggested that the truncated Myo1c IQ construct localized to similar regions as endogenous Myo1c. To further evaluate the importance of Myo1c domains in targeting, we determined the distribution of three Myo1c EGFP constructs (Fig. 1), full-length, IQ (lacking ATP and actin domains), and Tail (lacking ATP, actin and first 3 IQ motifs), transfected into M1 cells. Figure 8 shows confocal planes of M1 cells transiently transfected with EGFP-Myo1c full-length construct (Fig. 8, A, D, and G), IQ construct (Fig. 8, B, E, and H), or Tail construct (Fig. 8, C, F, and I). Figure 8, Az, Bz, and Cz, are x -z cuts of Fig. 8, A-C, respectively. Figure 8, D-F, are x -z images, whereas Fig. 8, G-I, are low-power x -y planes. In each case the EGFP was present on the amino end of the Myo1c construct. Not surprisingly, based on our M1IQ immunofluorescence results, both the full-length and IQ constructs were often observed to be concentrated in proximity to the plasma membrane. This was consistent with the IQ construct containing a domain sufficient for membrane targeting, as we observed in LLC-PK cells (57). These results are also consistent with the observations in hair cells that support the importance of the IQ region in Myo1c targeting (16). In contrast, the Tail construct, which lacked IQ domains 1-3, was not located at the plasma membrane and appeared to have a predominantly cytosolic distribution.

Does expression of truncated Myo1c alter tight junction structure and are there ultrastructural changes in the M1IQ cells? The electrophysiological experiments indicated that the stably transfected M1IQ and MF3 cells had a significantly reduced resistance compared with the M1 parent line. In an effort to better understand what might be causing this differ-

ence we evaluated the distribution of the tight junction component ZO-1. Similar and typical ZO-1 staining was observed in both cells. To further evaluate any structural abnormalities between M1 and M1IQ cells, filter-grown cells were fixed and processed for electron microscopy. These initial studies did not show any significant ultrastructural differences.

DISCUSSION

The proper placement, function, and regulation of membrane channels, receptors, and transporters are vital to physiological function. The delivery of these proteins to the plasma membrane is a vesicle-dependent process that must migrate through the actin-rich cortex (10). Epithelial cells, such as collecting duct cells, have evolved intricate pathways to both deliver and regulate multiple channels on both their apical and basolateral membranes (1, 4, 6, 13, 25, 32, 39-41, 48). The importance of actin and actin-associated proteins is well established, although the precise mechanisms of their action(s) require further investigation. We propose that Myo1c is, or becomes, an integral part of a channel-associated domain after a cell stimulus. This would provide the channel complex with an ATP- and Ca^{2+} -regulated motor that could modulate the spatial organization of specific channels and their effectors. By actively concentrating channel effectors, both proteins and lipids, Myo1c would facilitate the creation of a selective channel effector complex able to respond quickly to the physiological cell environment. Myo1c regulation could take place via tightly controlled calcium changes that modulate its multiple calmodulin-binding IQ region associations (16). Additional control of Myo1c activity and associations may involve phosphorylation events and specific membrane interactions.

In these studies we have addressed the function of an unconventional myosin I, Myo1c, in collecting duct cells. The model used was the well-established M1 mouse cortical collecting duct cell line. Our working hypothesis was that ENaC channel insertion is dependent on actin-Myo1c interactions. The delivery and insertion of ENaC channels to the plasma

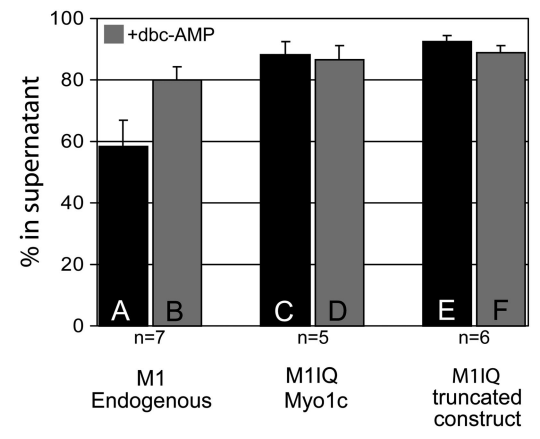


Fig. 7. Solubility of Myo1c after cAMP increase and/or in the presence of truncated Myo1c. Filter-grown cells were extracted with Triton X-100 under control conditions (A, C, E) and after stimulation of cells with 1 mM DBcAMP for 2 min (B, D, F). Samples were centrifuged at 100,000 g for 30 min, and supernatant and pellets were examined for endogenous Myo1c and truncated Myo1c with Western blot techniques. Western blots were scanned and quantitated, and percent Myo1c in the supernatant is shown. A-D: percentage of endogenous Myo1c in M1 and M1IQ cells. E and F: location of the truncated construct in the M1IQ cells. Error bars represent SE.

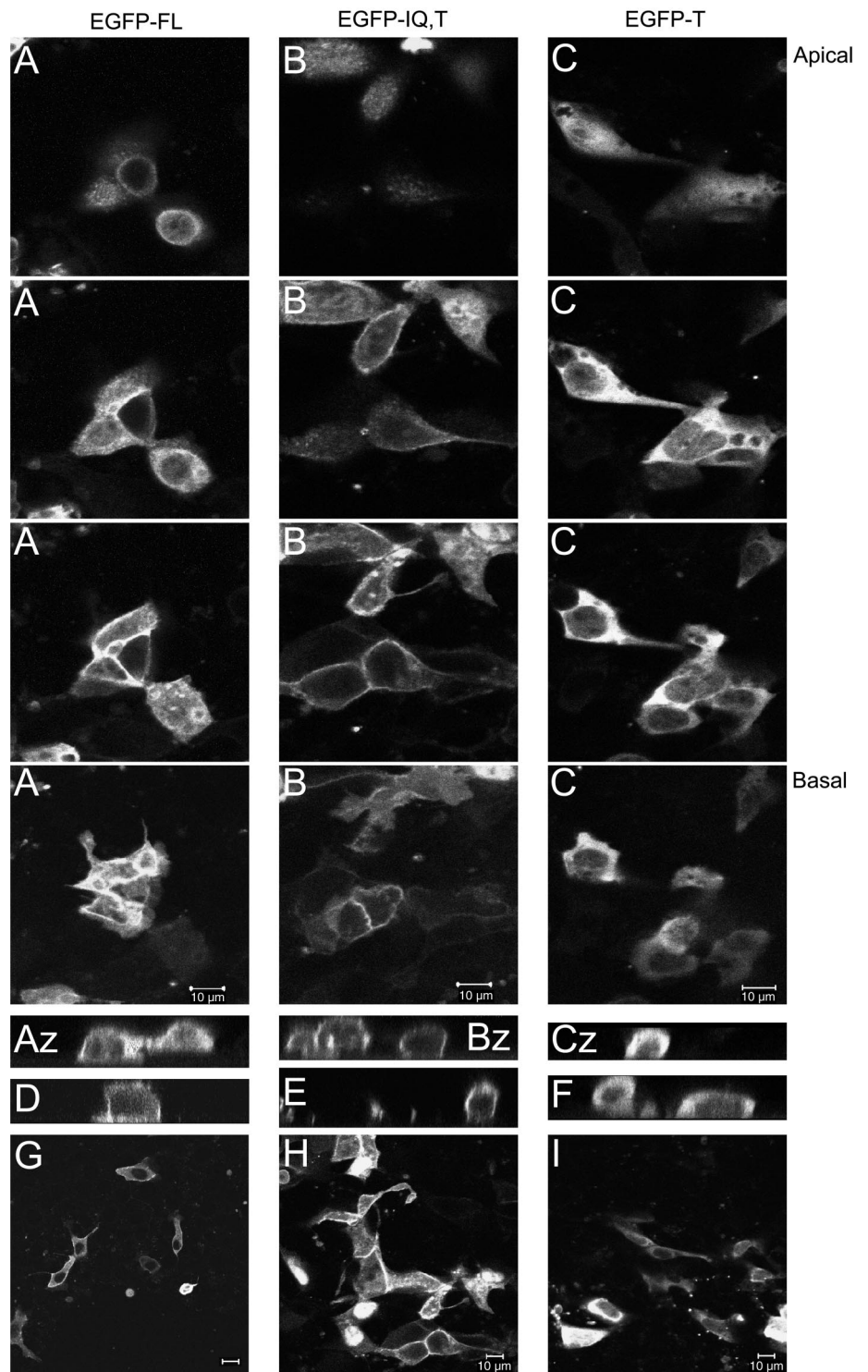


Fig. 8. Transient transfection of M1 cells with EGFP-Myo1c constructs. Confocal image planes from live M1 cells transiently transfected with EGFP-Myo1c full-length constructs (A, D, G), EGFP-Myo1c IQ construct (B, E, H), or EGFP-Myo1c Tail construct (C, F, I) are shown. Four representative planes from apical to basal are presented for A–C. An *x-z* plane is also shown (Az, Bz, Cz). D–F: additional *x-z* cuts from each of the respective constructs. G–I: another single *x-y* plane of each of the constructs. Myo1c full-length and IQ constructs are located in close proximity to the plasma membrane, consistent with our immunofluorescence data (Fig. 3). In contrast, the Myo1c Tail construct has a more cytoplasmic distribution.

membrane after ADH stimulation is well established (18, 48). In contrast, ADH and subsequent cAMP increase is thought to cause both the activation of existing CFTR plasma membrane channels and the insertion of new channels (4). Our approach compared the responses of parental cells to those of cells stably expressing a truncated, motor domain-deleted Myo1c and cells overexpressing Myo1c. Myo1c, as well as the truncated construct, was found to be concentrated at the plasma membrane,

often in discrete domains. Expression of truncated Myo1c modulated the ADH response, and these cells had a diminished amiloride inhibition. Surprisingly, expression of the full-length construct also resulted in an altered ADH response and diminished amiloride inhibition. These results are consistent with these cells having diminished ENaC plasma membrane delivery and/or activation. The observed increase in SCC after DBcAMP addition likely represents Cl⁻ movement, possibly



via CFTR. Understanding this change that occurs in the presence of amiloride will require further investigation. The M1IQ cell alterations observed may be the result of incorporation of truncated Myo1c into endogenous Myo1c complexes. The truncated construct would be unable to perform any mechanochemical function and might also disrupt Myo1c's normal protein or lipid associations that occur during activation of channels. The MF3 cells, which overexpress Myo1c, have a much higher basal SCC in addition to ADH and amiloride responses similar to the M1IQ cells. The two most likely explanations for the high basal SCC are increased channel density and increased activation of channels. In either case, the overexpression of Myo1c appears to have resulted in altered channel regulation whereby some channels are preferentially inserted or active at the plasma membrane while the ADH-responsive Na⁺ channel is reduced. Deciphering which channel(s) is responsible for the MF3 cell basal SCC will contribute to a better understanding of how Myo1c contributes to the complex cytoskeleton regulation of channel activity.

The identification of Myo1c binding partners has been difficult, with recent studies suggesting that the IQ domain is important (16). In fact, in expressed Myo1c fragments, Gillespie's results (16) in hair cells suggest that the second IQ domain must release calmodulin before receptor binding. Our studies with EGFP-Myo1c constructs show that the EGFP-Myo1cIQ construct does, indeed, colocalize to the same cell regions along the plasma membrane as the full-length construct. However, the EGFP-tail construct that lacks both the motor and IQ domains is present in a diffuse cytoplasmic pattern. Also, in agreement with our immunofluorescence results, none of the EGFP-Myo1c constructs localized to any actin stress fibers. Myo1c may be selectively targeted to specific actin areas by actin-associated proteins, such as tropomyosin, that prevent or possibly promote Myo1c actin binding.

The effect of calcium on myosin I's calmodulin and phospholipid interactions was first studied with brush border myosin I. Swanlung-Collins and Collins (51) proposed a calmodulin/phosphatidylserine switch whereby at micromolar calcium concentrations a calmodulin was released with an increase in lipid binding. A more recent study using expressed Myo1c tail protein suggested that calcium decreases Myo1c lipid association (52). It is also clear that both Myo1c's actin motility and actin-dependent ATPase activity are affected by calcium (3, 60). The regulation of Myo1c is likely to have both common and unique parameters that are dictated by cell type. In the collecting duct, one possibility is that on cell stimulation a local calcium increase causes the release of one calmodulin molecule from Myo1c, thus revealing a new protein-binding site. Another possibility may involve a change in the IQ domain conformation resulting from lipid binding to the tail domain. The release of calmodulin from Myo1c may also contribute to the regulation of other calmodulin-binding proteins. Where and when Myo1c releases and binds calmodulin are important questions that require further investigation.

Myo1c regulation of a channel or channel effector complex near the plasma membrane would likely involve movement or rearrangement of the cortical actin cytoskeleton. Two possible mechanisms by which Myo1c could alter ion channel properties include altering channel insertion into plasma membrane and altering the cortical actin cytoskeleton, which indirectly affects the channel's properties. Actin-dependent motility

would follow calmodulin release and receptor-cargo binding initiating delivery of cargo to membrane domains or modulation of cortical actin cytoskeleton, thus resulting in full activation of the channel. Alternatively, Myo1c actions may result in inhibition of activity by preventing necessary protein or lipid interactions. Phosphorylation of Myo1c will likely have a role in its activity and interactions. Regulation of cargo interaction by phosphorylation may be a common mechanism used by molecular motors (27, 48). It is possible that a phosphorylation event on Myo1c serves as the brake or signal once the necessary cortical cytoskeleton or membrane movement has occurred. The kinase and phosphatase that are responsible may be spatially restricted, thus contributing to the regulation of these events. The cessation of myosin actin-based motility may also have a filament-based component, as actin bound with tropomyosin significantly reduces myosin I-based activity and motility (19).

A recurring theme involving complex signaling pathways is establishment of specific domains or assemblies of proteins that raise the local concentration of each protein and any signaling intermediates that may be generated (23). This not only reduces the distance needed for communication but enables faster responses and allows multiple signaling events to take place with less cross talk. Detergent-resistant membranes, i.e., lipid rafts and caveolae, can serve as assembly sites for channels and effectors, thus facilitating interactions and activity (47, 59). Interestingly, ENaC and Myo1c both associate with anionic phospholipids (34, 52).

These results, combined with the results of earlier studies, provide compelling evidence that Myo1c is an important actin-dependent motor protein that participates in the modulation of ENaC in M1 cells. M1 cells expressing a truncated Myo1c, lacking ATP- and actin-binding domains, have altered SCC when stimulated with ADH, which has been shown to result in ENaC insertion into the plasma membrane. Ion channel function depends on insertion and removal of channels from the plasma membrane in addition to specific activation signals. Many of these events take place near or within the cortical actin cytoskeleton, which has been implicated in controlling a diverse array of channels. Our hypothesis is that Myo1c, through its interactions with actin, membranes and membrane binding proteins, and calmodulin is a key regulator of these events for ENaC. Live cell imaging of fluorescently tagged channels in cells expressing Myo1c mutations will help to clarify Myo1c's contribution to channel function.

ACKNOWLEDGMENTS

The authors thank Dr. Martin Bahler for the Myr2 plasmid, Charity Nofziger for assistance with the electrophysiological experiments, and Dr. Robert Bacallao for advice on extraction of filter-grown cells. Continued support by Dr. Bruce Molitoris and other members of the Nephrology Division is also appreciated.

Present address of A. Srirangam: Dept. of Hematology/Oncology, Indiana University School of Medicine, Indianapolis, IN 46202.

GRANTS

This work was supported by National Institute of Diabetes and Digestive and Kidney Diseases Grant DK-54923 (to M. C. Wagner).

REFERENCES

1. Apodaca G. Modulation of membrane traffic by mechanical stimuli. *Am J Physiol Renal Physiol* 282: F179–F190, 2002.



2. Barylko B, Binns DD, and Albanesi JP. Regulation of the enzymatic and motor activities of myosin I. *Biochim Biophys Acta* 1496: 23–35, 2000.
3. Barylko B, Wagner MC, Reizes O, and Albanesi JP. Purification and characterization of a mammalian myosin I. *Proc Natl Acad Sci USA* 89: 490–494, 1992.
4. Bertrand CA and Frizzell RA. The role of regulated CFTR trafficking in epithelial secretion. *Am J Physiol Cell Physiol* 285: C1–C18, 2003.
5. Blazer-Yost BL, Butterworth M, Hartman AD, Parker GE, Faletti CJ, Els WJ, and Rhodes SJ. Characterization and imaging of A6 epithelial cell clones expressing fluorescently labeled ENaC subunits. *Am J Physiol Cell Physiol* 281: C624–C632, 2001.
6. Blazer-Yost BL, Esterman MA, and Vlahos CJ. Insulin-stimulated trafficking of ENaC in renal cells requires PI 3-kinase activity. *Am J Physiol Cell Physiol* 284: C1645–C1653, 2003.
7. Bose A, Guilherme A, Robida SI, Nicoloso SM, Zhou QL, Jiang ZY, Pomerleau DP, and Czech MP. Glucose transporter recycling in response to insulin is facilitated by myosin Myo1c. *Nature* 420: 821–824, 2002.
8. Bose A, Robida S, Furcinitti PS, Chawla A, Fogarty K, Corvera S, and Czech MP. Unconventional myosin Myo1c promotes membrane fusion in a regulated exocytic pathway. *Mol Cell Biol* 24: 5447–5458, 2004.
9. Boyd-White J, Srirangam A, Goheen MP, and Wagner MC. Ischemia disrupts myosin Iβ in renal tubules. *Am J Physiol Cell Physiol* 281: C1326–C1335, 2001.
10. Brown D and Stow JL. Protein trafficking and polarity in kidney epithelium: from cell biology to physiology. *Physiol Rev* 76: 245–297, 1996.
11. Cantiello HF. Role of the actin cytoskeleton on epithelial Na⁺ channel regulation. *Kidney Int* 48: 970–984, 1995.
12. Catlett NL, Dux JE, Tang F, and Weisman LS. Two distinct regions in a yeast myosin-V tail domain are required for the movement of different cargoes. *J Cell Biol* 150: 513–526, 2000.
13. Chou CL, Yip KP, Michea L, Kador K, Ferraris JD, Wade JB, and Knepfer MA. Regulation of aquaporin-2 trafficking by vasopressin in the renal collecting duct. Roles of ryanodine-sensitive Ca²⁺ stores and calmodulin. *J Biol Chem* 275: 36839–36846, 2000.
14. Cordonnier MN, Dauzonne D, Louvard D, and Coudrier E. Actin filaments and myosin I alpha cooperate with microtubules for the movement of lysosomes. *Mol Biol Cell* 12: 4013–4029, 2001.
15. Cox D, Berg JS, Cammer M, Chingwundoh JO, Dale BM, Cheney RE, and Greenberg S. Myosin X is a downstream effector of PI(3)K during phagocytosis. *Nat Cell Biol* 4: 469–477, 2002.
16. Cyr JL, Dumont RA, and Gillespie PG. Myosin-1c interacts with hair-cell receptors through its calmodulin-binding IQ domains. *J Neurosci* 22: 2487–2495, 2002.
17. Durrbach A, Raposo G, Tenza D, Louvard D, and Coudrier E. Truncated brush border myosin I affects membrane traffic in polarized epithelial cells. *Traffic* 1: 411–424, 2000.
18. Els WJ and Helman SI. Dual role of prostaglandins (PGE₂) in regulation of channel density and open probability of epithelial Na⁺ channels in frog skin (*R. pipiens*). *J Membr Biol* 155: 75–87, 1997.
19. Fanning AS, Wolenski JS, Mooseker MS, and Izant JG. Differential regulation of skeletal muscle myosin-II and brush border myosin-I enzymology and mechanochemistry by bacterially produced tropomyosin isoforms. *Cell Motil Cytoskeleton* 29: 29–45, 1994.
20. Garcia JA, Yee AG, Gillespie PG, and Corey DP. Localization of myosin-Iβ near both ends of tip links in frog saccular hair cells. *J Neurosci* 18: 8637–8647, 1998.
21. Gillespie PG and Corey DP. Myosin and adaptation by hair cells. *Neuron* 19: 955–958, 1997.
22. Gillespie PG, Wagner MC, and Hudspeth AJ. Identification of a 120 kd hair-bundle myosin located near stereociliary tips. *Neuron* 11: 581–594, 1993.
23. Hille B. *Ion Channel of Excitable Membranes*. Sunderland, MA: Sinauer, 2001.
24. Howard DP, Cuffe JE, Boyd CA, and Korbmacher C. L-arginine effects on Na⁺ transport in M-1 mouse cortical collecting duct cells—a cationic amino acid absorbing epithelium. *J Membr Biol* 180: 111–121, 2001.
25. Huber LA, Fialka I, Paiha K, Hunziker W, Sacks DB, Bahler M, Way M, Gagescu R, and Gruenberg J. Both calmodulin and the unconventional myosin Myr4 regulate membrane trafficking along the recycling pathway of MDCK cells. *Traffic* 1: 494–503, 2000.
26. Jentsch TJ, Stein V, Weinreich F, and Zdebek AA. Molecular structure and physiological function of chloride channels. *Physiol Rev* 82: 503–568, 2002.
27. Karcher RL, Deacon SW, and Gelfand VI. Motor-cargo interactions: the key to transport specificity. *Trends Cell Biol* 12: 21–27, 2002.
28. Koefoed-Johnsen V and Ussing HH. The nature of the frog skin potential. *Acta Physiol Scand* 42: 298–308, 1958.
29. Korbmacher C, Segal AS, Fejes-Toth G, Giebisch G, and Boulpaep EL. Whole-cell currents in single and confluent M-1 mouse cortical collecting duct cells. *J Gen Physiol* 102: 761–793, 1993.
30. Lahr TF, Record RD, Hoover DK, Hughes CL, and Blazer-Yost BL. Characterization of the ion transport responses to ADH in the MDCK-C7 cell line. *Pflügers Arch* 439: 610–617, 2000.
31. Letz B and Korbmacher C. cAMP stimulates CFTR-like Cl⁻ channels and inhibits amiloride-sensitive Na⁺ channels in mouse CCD cells. *Am J Physiol Cell Physiol* 272: C657–C666, 1997.
32. Loffing-Cueni D, Loffing J, Shaw C, Taplin AM, Govindan M, Stanton CR, and Stanton BA. Trafficking of GFP-tagged ΔF508-CFTR to the plasma membrane in a polarized epithelial cell line. *Am J Physiol Cell Physiol* 281: C1889–C1897, 2001.
33. Louvard D. Polarity of epithelial cells. Role of the actin microfilament system. *Nephrologie* 17: 351–357, 1996. (In French.)
34. Ma HP, Saxena S, and Warnock DG. Anionic phospholipids regulate native and expressed epithelial sodium channel (ENaC). *J Biol Chem* 277: 7641–7644, 2002.
35. Mall M, Bleich M, Kuehr J, Brandis M, Greger R, and Kunzelmann K. CFTR-mediated inhibition of epithelial Na⁺ conductance in human colon is defective in cystic fibrosis. *Am J Physiol Gastrointest Liver Physiol* 277: G709–G716, 1999.
36. Maunsbach AB and Afzelius BA. *Biomedical Electron Microscopy*. San Diego, CA: Academic, 1999.
37. Meyer K and Korbmacher C. Cell swelling activates ATP-dependent voltage-gated chloride channels in M-1 mouse cortical collecting duct cells. *J Gen Physiol* 108: 177–193, 1996.
38. Ostap EM and Pollard TD. Biochemical kinetic characterization of the Acanthamoeba myosin-I ATPase. *J Cell Biol* 132: 1053–1060, 1996.
39. Peters KW, Qi J, Johnson JP, Watkins SC, and Frizzell RA. Role of snare proteins in CFTR and ENaC trafficking. *Pflügers Arch* 443: S65–S69, 2001.
40. Qualmann B, Kessels MM, and Kelly RB. Molecular links between endocytosis and the actin cytoskeleton. *J Cell Biol* 150: F111–F116, 2000.
41. Reid JM and O’Neil RG. Osmomechanical regulation of membrane trafficking in polarized cells. *Biochem Biophys Res Commun* 271: 429–434, 2000.
42. Ruppert C, Godel J, Muller RT, Kroschewski R, Reinhard J, and Bahler M. Localization of the rat myosin I molecules myr 1 and myr 2 and in vivo targeting of their tail domains. *J Cell Sci* 108: 3775–3786, 1995.
43. Schnermann JB and Sayegh SI. *Kidney Physiology*. Philadelphia, PA: Lippincott-Raven, 1998.
44. Schultz BD, Singh AK, Devor DC, and Bridges RJ. Pharmacology of CFTR chloride channel activity. *Physiol Rev* 79: S109–S144, 1999.
45. Schwiebert EM, Benos DJ, Egan ME, Stutts MJ, and Guggino WB. CFTR is a conductance regulator as well as a chloride channel. *Physiol Rev* 79: S145–S166, 1999.
46. Schwiebert EM, Mills JW, and Stanton BA. Actin-based cytoskeleton regulates a chloride channel and cell volume in a renal cortical collecting duct cell line. *J Biol Chem* 269: 7081–7089, 1994.
47. Shlyonsky VG, Mies F, and Sariban-Sohraby S. Epithelial sodium channel activity in detergent-resistant membrane microdomains. *Am J Physiol Renal Physiol* 284: F182–F188, 2003.
48. Smith PR. cAMP-mediated regulation of amiloride-sensitive sodium channels: channel activation or channel recruitment? In: *Amiloride-Sensitive Sodium Channels: Physiology and Functional Diversity*, edited by Benos DJ and Fambrough DM. San Diego, CA: Academic, 1999, p. 133–154.
49. Stachelek SJ, Kowalik TF, Farwell AP, and Leonard JL. Myosin V plays an essential role in the thyroid hormone-dependent endocytosis of type II iodothyronine 5'-deiodinase. *J Biol Chem* 275: 31701–31707, 2000.
50. Stoops BA, Naray-Fejes-Toth A, Carretero OA, Ito S, and Fejes-Toth G. Characterization of a mouse cortical collecting duct cell line. *Kidney Int* 39: 1168–1175, 1991.

51. **Swanlung-Collins H and Collins JH.** Brush border myosin I has a calmodulin/phosphatidylserine switch and tail actin-binding. *Adv Exp Med Biol* 358: 205–213, 1994.
52. **Tang N, Lin T, and Ostap EM.** Dynamics of Myo1c (myosin-I β) lipid binding and dissociation. *J Biol Chem* 277: 42763–42768, 2002.
53. **Todd-Turla KM, Rusvai E, Naray-Fejes-Toth A, and Fejes-Toth G.** CFTR expression in cortical collecting duct cells. *Am J Physiol Renal Fluid Electrolyte Physiol* 270: F237–F244, 1996.
54. **Wagner MC, Barylko B, and Albanesi JP.** Tissue distribution and subcellular localization of mammalian myosin I. *J Cell Biol* 119: 163–170, 1992.
55. **Wagner MC and Molitoris BA.** ATP depletion alters myosin I β cellular location in LLC-PK1 cells. *Am J Physiol Cell Physiol* 272: C1680–C1690, 1997.
56. **Wagner MC and Molitoris BA.** Renal epithelial polarity in health and disease. *Pediatr Nephrol* 13: 163–170, 1999.
57. **Wagner MC, Srirangam A, and Boyd-White J.** Analysis of myosin I β -GFP constructs expressed in multiple cell types (Abstract). *Mol Biol Cell* 11: 164a, 2000.
58. **Yamoah EN, Lumpkin EA, Dumont RA, Smith PJ, Hudspeth AJ, and Gillespie PG.** Plasma membrane Ca²⁺-ATPase extrudes Ca²⁺ from hair cell stereocilia. *J Neurosci* 18: 610–624, 1998.
59. **Zajchowski LD and Robbins SM.** Lipid rafts and little caves. Compartmentalized signalling in membrane microdomains. *Eur J Biochem* 269: 737–752, 2002.
60. **Zhu T, Sata M, and Ikebe M.** Functional expression of mammalian myosin I β : analysis of its motor activity. *Biochemistry* 35: 513–522, 1996.

